NACA

RESEARCH MEMORANDUM

DRAG OF EXTERNAL STORES AND NACELLES AT TRANSONIC AND SUPERSONIC SPEEDS

By Norman F. Smith, Ralph P. Bielat, and Lawrence D. Guy

Langley Aeronautical Laboratory
Langley Field, Va.

NATIONAL ADVISORY COMMITTEE
FOR AERONAUTICS

WASHINGTON
October 29, 1953

NATIONAL ADVISORY COMMITTEE FOR AERONAUTICS

RESEARCH MEMORANDUM

DRAG OF EXTERNAL STORES AND NACELLES AT TRANSONIC AND SUPERSONIC SPEEDS

By Norman F. Smith, Ralph P. Bielat, and Lawrence D. Guy

INTRODUCTION

The problem of designing nacelles and stores is one of providing the desired volume in an acceptable shape or position at the lowest possible cost in airplane performance. There is considerable evidence that such volume can often be more efficiently carried within the basic wing-body combination, especially at supersonic flight speeds. Discussion of submerged or integral arrangements, however, involves complex design studies which are beyond the scope of this paper. This paper deals entirely with external stores and nacelles, primarily wing-mounted on airplane-type configurations.

The complexity of the flow field about a configuration at supersonic and particularly at transonic speeds with shock interaction and interference, local choking, separation, and so forth, makes theoretical treatment of the interference problem very difficult. For this reason, the main approach to the problem has been experimental, with a substantial amount of experimental research having been done on external store and nacelle configurations.

Only to a very limited extent, however, has satisfactory analysis of store or nacelle drag on the basis of position been feasible. Unexplained trends and seemingly contradictory results between several investigations along with the large number of configuration variables involved have made generalized experimental investigation difficult and have tended to make the results rather specific in nature.

It is therefore of interest to apply a simplifying principle, such as the transonic area rule discussed in reference 1. Consequently, the bulk of the transonic data which have been obtained on stores and nacelles, most of which have been published and analyzed with respect to spanwise and chordwise positions, has been reexamined in the light of the area rule in the present report. Also, the available supersonic data have been subjected to an exploratory analysis based upon the supersonic area rule (ref. 2).

DISCUSSION

In order to show the general situation with regard to experimental data, a plot of drag coefficient based upon individual frontal area against Mach number is presented in figure 1. The shaded areas show the Mach numbers and drag-coefficient values corresponding to nacelles and stores which have been investigated to date. All these data have been published. The publications which are used in detail in this paper are listed as references 3 to 16. The values of drag coefficient which have been obtained in the transonic range vary from above 0.8 to near zero. At the three higher supersonic Mach numbers, the values vary from nearly 0.8 to around 0.23. The lower shaded band shows the range of drag values covered by isolated-body drags for satisfactory supersonic bodies of fineness ratio of approximately 6 to 9, (refs. 3, 4, and others). This figure shows that zero interference and even greatly beneficial interference have been obtained on configurations in the transonic range up to $M = 1.2$ (refs. 5, 6, and 7, for example). Apparently, however, no beneficial interference has yet been encountered with airplane-type configurations at the three higher supersonic Mach numbers shown, and only in a few cases has interference near zero been attained. It should be noted here that nacelle drags near zero have in some cases been obtained for large ram-jet nacelles mounted on missile configurations (ref. 8). This large favorable interference was obtained in extreme rearward positions wherein half the nacelle length extended beyond the fuselage base, positions very different from those used for airplane nacelles. (Further evidence of large favorable interference for nacelles in this region has been found in the theoretical work of ref. 9.)

The store and nacelle data which make up these shaded areas have been examined in detail to determine some of the factors which govern the drag of these installations.

Transonic Speeds

Figure 2 shows the transonic drag-rise data for the series of spanwise symmetrically mounted nacelles tested in flight by the Langley Pilotless Aircraft Research Division on a 45° swept wing of aspect ratio 6, $t/c = 0.09$ (ref. 7). On the right-hand side of the figure is a sketch which shows the location of the nacelle and a diagram of the cross-sectional area variation of each configuration. In this figure and in figures 3 and 4, the data are plotted as drag increments above the level for $M = 0.8$ in order to eliminate the skin-friction drag. Figure 2 shows that the highest drag rise is obtained with the nacelle position giving the highest peak on the area diagram and the highest slopes forward and aft. The lowest drag is obtained with the nacelle position which affects the wing-body area diagram least. In looking at the

transonic drag rises in terms of spanwise variation of nacelle position, it is noted that the drag is least at the tip, rises to a peak value at 0.4b/2, and decreases again as the nacelle is moved still farther inward to 0.18b/2. This phenomenon had thus far gone unexplained. The area rule provides, in this case and others to be mentioned subsequently, a simple explanation. It will be noted that the differences between the drag curves are small. This is a result of the fact that these nacelles are small, corresponding roughly to single-engine units.

Figures 3 and 4 show similar results obtained from wind-tunnel tests conducted in the Langley 8-foot transonic tunnel and 4- by 4-foot supersonic pressure tunnel (refs. 10 to 13 and some unpublished data) of a sting-mounted configuration involving a series of nacelles of twin-engine size on a swept wing of aspect ratio 3.5 with 47° sweep and a thickness ratio of 6 percent. The series shown in figure 3 is a family of pylon-mounted nacelles which involves a forward and downward movement at one spanwise station, and the series in figure 4 consists of different types of nacelles. Again correlation with the area diagram is clear, with the top configurations having the least favorable area diagrams and the highest transonic drag rises.

The equivalent stream-tube area corresponding to the internal flow has been subtracted from the areas shown in figure 4. Note the particularly low drag rise for the installation buried in the wing root with provisions for air intake at the leading edge. This installation is actually more a submerged installation than an external one but is shown here because of its excellent drag characteristics and because it was a part of the test series. Plots of drag-rise data for the configurations shown in these two figures at lift coefficients up to 0.5 have been made and show that the curves maintain the same relationship to each other as do the curves shown here for $C_L = 0$.

Examination of the nacelle and store information from the Langley Pilotless Aircraft Research Division, 7- by 10-foot tunnels, and 8-foot transonic tunnel shows area-diagram correlations consistent with those shown in these three examples.

The dashed lines in figures 3 and 4 connect the limited number of supersonic points which are available for some of these configurations. The supersonic points in figure 3 show that the high drag levels obtained transonically do not necessarily persist into the supersonic speed range. The indication is thus that the requirements for low wave drag in the transonic range may be different from those in the supersonic speed range. The supersonic range will be treated in more detail subsequently.

Because interpretation of area diagrams tends to become somewhat indefinite in some cases, a very simple parameter concerning the area

diagram has been devised. In figure 5 the data from the series of different nacelles and the series of pylon-mounted nacelles, most of which were shown in figures 3 and 4, have been plotted as incremental drag coefficients against x/l, where x is the distance from the area peak of the wing-fuselage combination to the area peak of the complete-model configuration, the areas having been obtained by sectioning the models in planes perpendicular to the longitudinal axis. Data for $M = 1.0$ are shown at the left; data for $M = 1.1$, at the right. The $M = 1.1$ condition corresponds to the completion of the drag rise, while at $M = 1.0$ the drag values are still rising rapidly. The correlation at both Mach numbers is very good. A number of different nacelle configurations and different types of area diagrams are involved, as will be remembered from figures 3 and 4. The correlation shows that the highest drags are obtained when the area peaks coincide, with the drag decreasing rapidly as the area peaks are displaced. Note that the parameter used does not show effects of area coincidence alone. As the peaks are moved, slope changes forward and aft also occur. This parameter is therefore only one small step removed from visual interpretation of the area diagram.

Thus, by reanalysis of a large amount of nacelle and store data, it was found that correlation with the area rule is found for many types of nacelles or stores in positions from wing root to wing tip, and that explanation of phenomena not heretofore explained is afforded. Because the configurations considered were all designed without regard for the area rule, it is very difficult to extract quantitative data from this work. Changes in area-diagram characteristics from one configuration to another involve random simultaneous changes in peak height, local slopes, and over-all shapes. Controlled experiments are needed to provide valid quantitative data.

Proof of the importance of the area rule is strengthened by demonstration of its use in the design of configurations complete with nacelles. Figures 6 and 7 show unpublished results for two delta-wing configurations from wind-tunnel and flight tests by the Pilotless Aircraft Research Division. The configuration shown in the left side of figure 6 has an area diagram which shows a very high peak and high slopes forward and aft, due largely to the nacelles. The drag for this configuration is very high, as is the drag (plus interference) for the nacelles, obtained by subtraction. Data obtained in the Langley 16-foot transonic tunnel for the same configuration, but with air flow through the nacelles, show somewhat lower drag. The area diagram for this case, which is reduced by allowance for the equivalent stream-tube area through the nacelles, is shown by the long dashed lines.

A sketch of a second version of this configuration is shown in the right side of this figure. The wing was enlarged and thinned somewhat and the nacelles were split into forward and aft pairs. The fuselage was

lengthened and was undercut slightly in order to make the area diagram for the complete configuration correspond closely to a parabolic distribution of higher fineness ratio than the previous model. The drag curve shows a drag reduction for this configuration of nearly 50 percent, or 40 percent of the configuration at left with air flow. The nacelle contribution in this case is not known, but it is clear that a similar reduction in nacelle drag and interference has occurred.

Figure 7 shows that in both of these cases, the drag characteristics of the complete configuration are closely simulated by drag characteristics of the body of revolution having an equivalent longitudinal area development. The measured drags for the equivalent bodies have been corrected to the skin-friction level of the complete configuration in each case. The configuration at the left is one of the configurations discussed in reference 1 wherein the item of equivalent bodies was treated in some detail.

Supersonic Speeds

In the supersonic speed range, the bulk of the experimental data, which have been obtained in addition to the data from the Langley 4- by 4-foot supersonic pressure tunnel shown in figures 3 and 4, is that obtained in the Langley 9- by 12-inch supersonic blowdown tunnel (refs. 14 to 16). Figure 8 shows the configurations tested: a half-model fuselage with a semispan unswept, a 45° swept, and a 60° delta wing. The store is of the Douglas store shape and was tested with the store center of gravity in the locations shown on the sketches. The store and wing surfaces were tangent for those chordwise positions where the maximum thicknesses coincided and were separated by a very short pylon for other positions. The store size may be considered to correspond roughly to a single-engine nacelle on a large bomber airplane.

The data presented in figure 9 are plotted in the form of store-plus-interference drag C_{D_N} against spanwise position for $M = 1.41$ and 1.96. Data for $M = 1.62$ are also available and agree well with the other two Mach numbers but are omitted here for simplicity. The data show that, in general, for all three wing configurations, moving the store outward decreases the store drag. A similar plot of chordwise positions (fig. 10) shows that moving the store forward decreases the drag. Exceptions to these generalizations are evident, however, in the solid symbols connected by dashed lines for the swept and delta wings, for which positions the drag is a great deal lower than would be expected or predicted by a straight line drawn through the remaining symbols.

Attempts to correlate these and some unpublished data on the basis of nacelle position with respect to the wing leading edge, fuselage nose Mach line, wing local maximum thickness, to mention a few, all failed -

if any correlation was obtained it contained exceptions which could not be explained. This difficulty of correlating or generalizing is, of course, similar to that mentioned previously for nacelle and store studies at transonic speeds.

An extension of the transonic area rule was utilized in an attempt to correlate these data. The more complete supersonic theory, which involves sectioning the configuration by a series of planes tangent to Mach cones, has been described in reference 2.

The method used here, as an exploratory approach, involves only one set of the planes indicated by the theory; that is, parallel vertical planes which intersect the configuration plan form along Mach lines. It will be noted that the fuselage in this case employed a cylindrical afterbody. The fuselage nose, therefore, can affect the pressure drag of the nacelle and wing, but the nacelle and wing cannot appreciably affect the pressure drag of the fuselage afterbody. It therefore appeared that the principal lines of influence or interference were Mach lines originating at the fuselage center line and that sectioning or viewing the model along these particular Mach lines might correlate the principal variations. Figure 11 shows the results of the correlation. The drag data for all the configurations shown in figure 8 have been plotted against x/l, which is the area-peak displacement parameter defined in the sketch (top part of fig. 11). (x is the distance between the peak of the area diagram of the store and the peak of the area diagram of the wing-fuselage combination, the area diagrams being obtained by sectioning the semispan configuration along Mach lines in the lateral plane and plotting the cross-sectional area given by each slice at the intercept on the fuselage center line.)

Clearly, the data show a strong trend similar to the one shown in figure 5 for the transonic case. If located in a region where its area peak adds to the wing-fuselage peak (viewed along the Mach line), the store produces higher drag than if located a short distance forward or aft of the $x = 0$ point. It will be noted that data from three different wing configurations, a straight, a swept, and a delta wing, and data at three supersonic Mach numbers, 1.41, 1.62, and 1.96, are all included in this plot.

This correlation plot explains the low drag points which appeared to contradict the spanwise and chordwise trends shown in figures 9 and 10. The solid symbols to the right of $x/l = 0$ are for these configurations. These drag values are in proper positions as located by the area diagram parameter x/l, and the low drag is explained by area-peak displacement.

It will be noted that at neither end of the curve of figure 11 has a minimum drag been reached. This means that minimum drag values will be attained at more extreme forward or aft nacelle positions than those tested. Practical difficulties may appear, however, in using such positions for airplane configurations.

[redacted]

There is considerable scatter of points from the trend line which has been drawn through the data. Only a part of this scatter can be explained by the data-accuracy spread shown by the width of the trend line. Some scatter in any correlation of this kind is to be expected, inasmuch as it is not reasonable to expect a perfect explanation of a complicated flow condition in terms of this very simple parameter. There are a large number of details which can greatly affect the drag. These details are wing-fuselage and wing-nacelle junctures, the detail design of each component, the effects of localized shock patterns, and so forth. Such details would influence the pressure drags to some extent and would particularly influence the friction drag which is not included in the area rule.

It should be mentioned that attenuation of interference effects as bodies are separated is also involved in the supersonic case. This factor causes the pressure interference between store and fuselage to diminish as the store is moved tipward on the wing. This item is included in the complete treatment mentioned previously which considers all the planes. The interference problem in the case of the tipward store is reduced to one of local interference of a more familiar nature between wing and store.

CONCLUSIONS

The following conclusions are indicated:

1. The transonic area rule can be applied to configurations involving many kinds of stores or nacelles in locations from wing root to wing tip.

2. The area rule is shown to function at supersonic Mach numbers in a similar fashion, utilizing in this first analysis, sectioning vertically along Mach lines originating at the fuselage center line.

3. The appreciable scatter which is present in the area-rule correlations may be reduced in later refinements but will always be present because of detail conditions or differences. It is emphasized, therefore, that good detail design of components, junctures, and so forth, must be adhered to. The area rule then offers a useful means by which the designer may arrange or integrate these components into the complete configuration having the best possible area and drag characteristics.

4. Quantitative data are lacking in all correlations because this analysis was based upon previous investigations which were not planned for obtaining such data. Further research is needed, using the area

rule and other theory as a guide, to obtain quantitative design data on the interference and optimum location of stores and nacelles.

Langley Aeronautical Laboratory,
National Advisory Committee for Aeronautics,
Langley Field, Va., September 3, 1953.

[redacted]

REFERENCES

1. Whitcomb, Richard T.: Recent Results Pertaining to the Application of the "Area Rule." NACA RM L53I15a, 1953.

2. Jones, Robert T.: Theory of Wing-Body Drag at Supersonic Speeds. NACA RM A53H18a, 1953.

3. Jackson, H. Herbert, Rumsey, Charles B., and Chauvin, Leo T.: Flight Measurements of Drag and Base Pressure of a Fin-Stabilized Parabolic Body of Revolution (NACA RM-10) at Different Reynolds Numbers and at Mach Numbers From 0.9 to 3.3. NACA RM L50G24, 1950.

4. Hart, Roger G., and Katz, Ellis R.: Flight Investigations at High-Subsonic, Transonic, and Supersonic Speeds To Determine Zero-Lift Drag of Fin-Stabilized Bodies of Revolution Having Fineness Ratios of 12.5, 8.91, and 6.04 and Varying Positions of Maximum Diameter. NACA RM L9I30, 1949.

5. Welsh, Clement J., and Morrow, John D.: Effect of Wing-Tank Location on the Drag and Trim of a Swept-Wing Model As Measured in Flight at Transonic Speeds. NACA RM L50A19, 1950.

6. Silvers, H. Norman, and King, Thomas J., Jr.: A Small-Scale Investigation of the Effect of Spanwise and Chordwise Positioning of an Ogive-Cylinder Underwing Nacelle on the High-Speed Aerodynamic Characteristics of a 45° Sweptback Tapered-in-Thickness Wing of Aspect Ratio 6. NACA RM L52J22, 1952.

7. Pepper, William B., Jr., and Hoffman, Sherwood: Comparison of Zero-Lift Drags Determined by Flight Tests at Transonic Speeds of Symmetrically Mounted Nacelles in Various Spanwise Positions on a 45° Sweptback Wing and Body Combination. NACA RM L51D06, 1951.

8. Kremzier, Emil J., and Dryer, Murray: Aerodynamic Interference Effects on Normal and Axial Force Coefficients of Several Engine-Strut-Body Configurations at Mach Numbers of 1.8 and 2.0. NACA RM E52B21, 1952.

9. Friedman, Morris D.: Arrangement of Bodies of Revolution in Supersonic Flow To Reduce Wave Drag. NACA RM A51I20, 1951.

10. Driver, Cornelius: Aerodynamic Characteristics at Supersonic Speeds of a Series of Wing-Body Combinations Having Cambered Wings With an Aspect Ratio of 3.5 and a Taper Ratio of 0.2. Effect at M = 2.01 of Nacelle Shape and Position on the Aerodynamic Characteristics in Pitch of Two Wing-Body Combinations With 47° Sweptback Wings. NACA RM L52F03, 1952.

[redacted]

11. Hasel, Lowell E., and Sevier, John R., Jr.: Aerodynamic Characteristics at Supersonic Speeds of a Series of Wing-Body Combinations Having Cambered Wings With an Aspect Ratio of 3.5 and a Taper Ratio of 0.2. Effect at M = 1.60 of Nacelle Shape and Position on the Aerodynamic Characteristics in Pitch of Two Wing-Body Combinations With 47° Sweptback Wings. NACA RM L51K14a, 1952.

12. Bielat, Ralph P., and Harrison, Daniel E.: A Transonic Wind-Tunnel Investigation of the Effects of Nacelle Shape and Position on the Aerodynamic Characteristics of Two 47° Sweptback Wing-Body Configurations. NACA RM L52G02, 1952.

13. Carmel, Melvin M., and Fischetti, Thomas L.: A Transonic Wind-Tunnel Investigation of the Effects of Nacelles on the Aerodynamic Characteristics of a Complete Model Configuration. NACA RM L53F22a, 1953.

14. Jacobsen, Carl R.: Effects of Systematically Varying the Spanwise and Vertical Location of an External Store on the Aerodynamic Characteristics of an Unswept Tapered Wing of Aspect Ratio 4 at Mach Numbers of 1.41, 1.62, and 1.96. NACA RM L52F13, 1952.

15. Jacobsen, Carl R.: Effects of the Spanwise, Chordwise, and Vertical Location of an External Store on the Aerodynamic Characteristics of a 45° Sweptback Tapered Wing of Aspect Ratio 4 at Mach Numbers of 1.41, 1.62, and 1.96. NACA RM L52J27, 1953.

16. Jacobsen, Carl R.: Effects of the Spanwise, Chordwise, and Vertical Location of an External Store on the Aerodynamic Characteristics of a 60° Delta Wing at Mach Numbers of 1.41, 1.62, and 1.96. NACA RM L52H29, 1952.

EXPERIMENTAL EXTERNAL-STORE AND NACELLE DRAGS

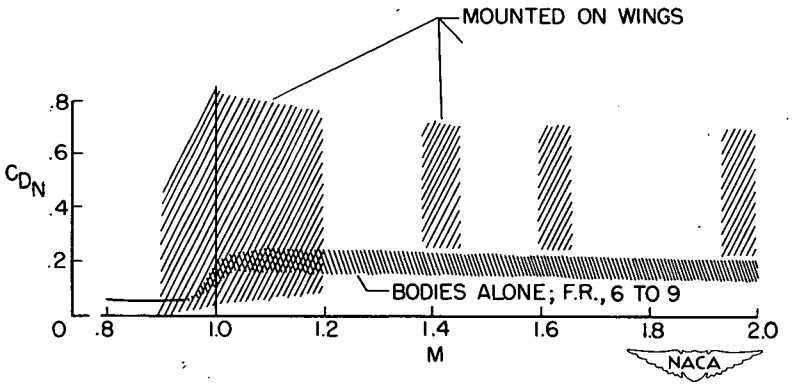

Figure 1

DRAG OF SPANWISE SERIES OF SYMMETRICALLY MOUNTED NACELLES

$C_L = 0$

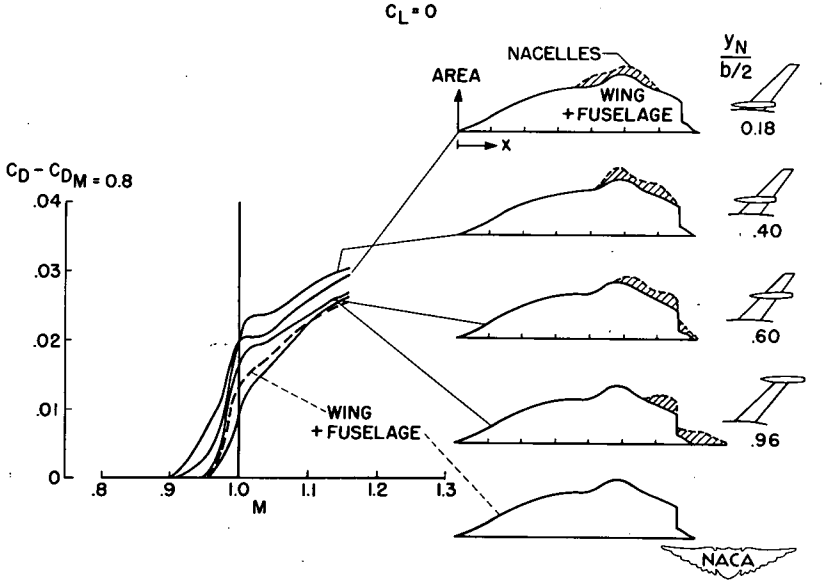

Figure 2

[redacted]

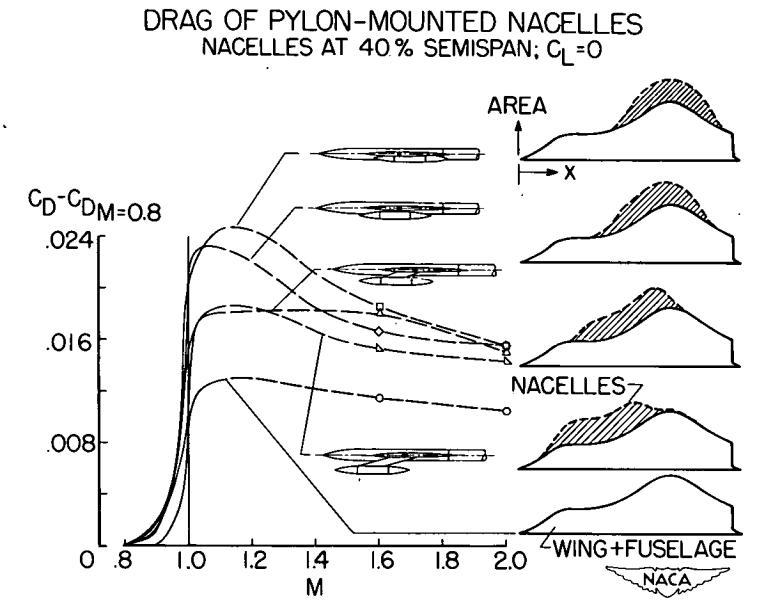

Figure 3

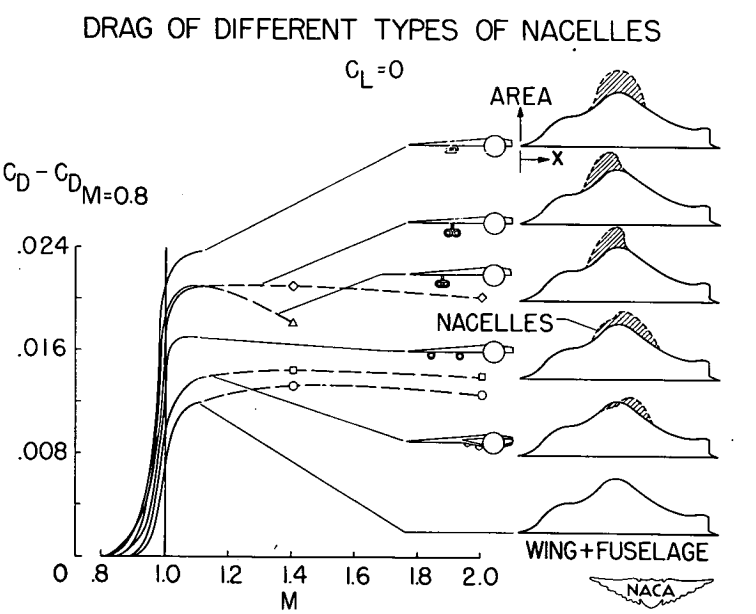

Figure 4

[redacted]

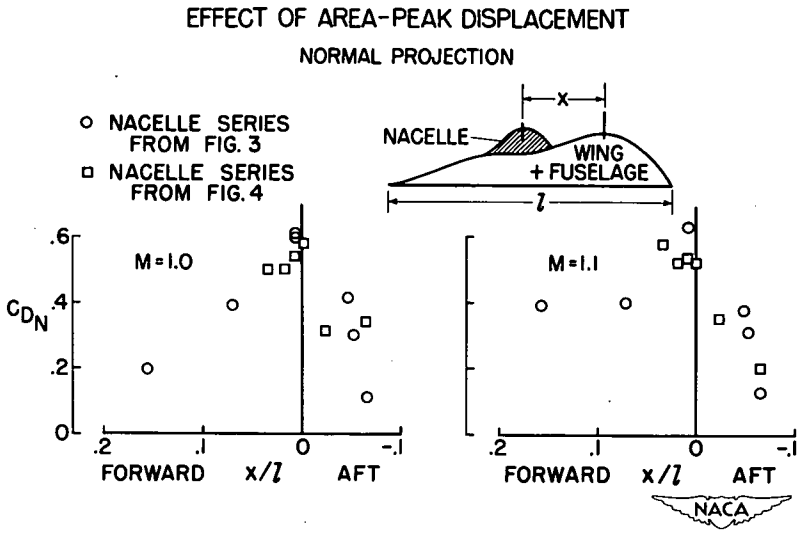

Figure 5

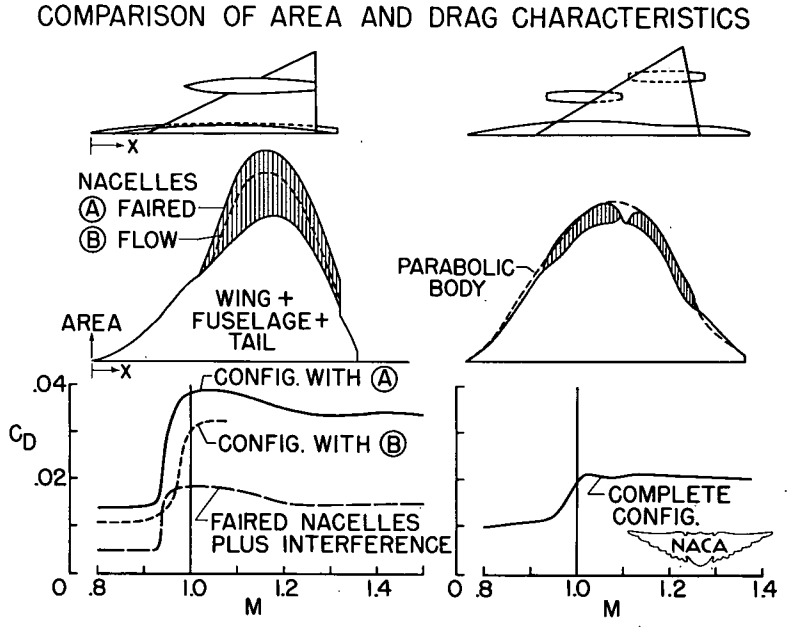

Figure 6

DRAG OF COMPLETE CONFIGURATIONS AND EQUIVALENT BODIES

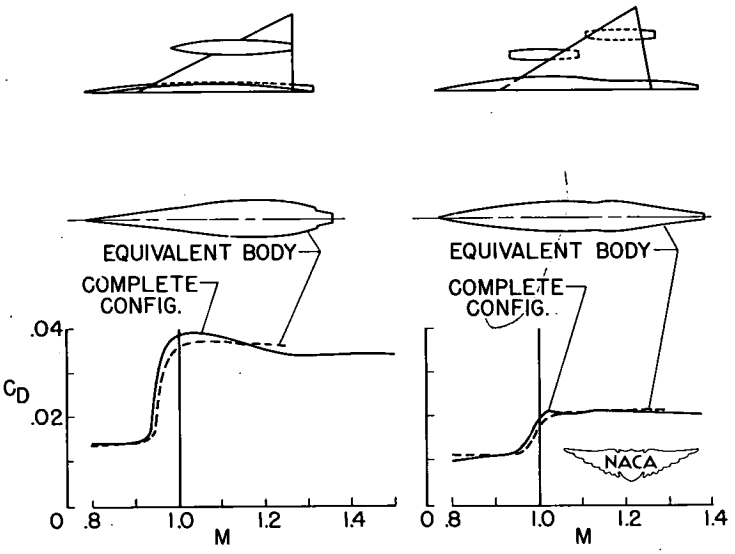

Figure 7

WING FUSELAGE, AND STORE GEOMETRY

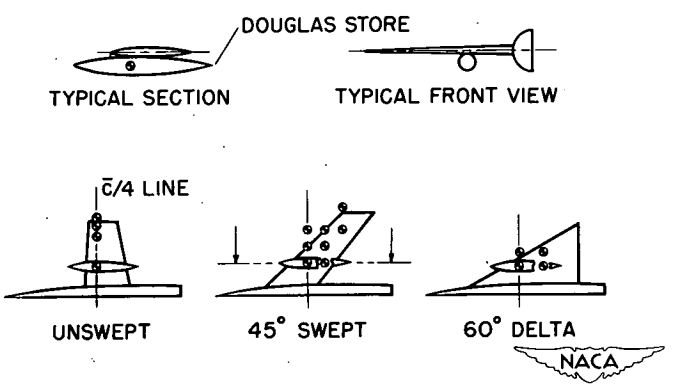

Figure 8

[redacted]

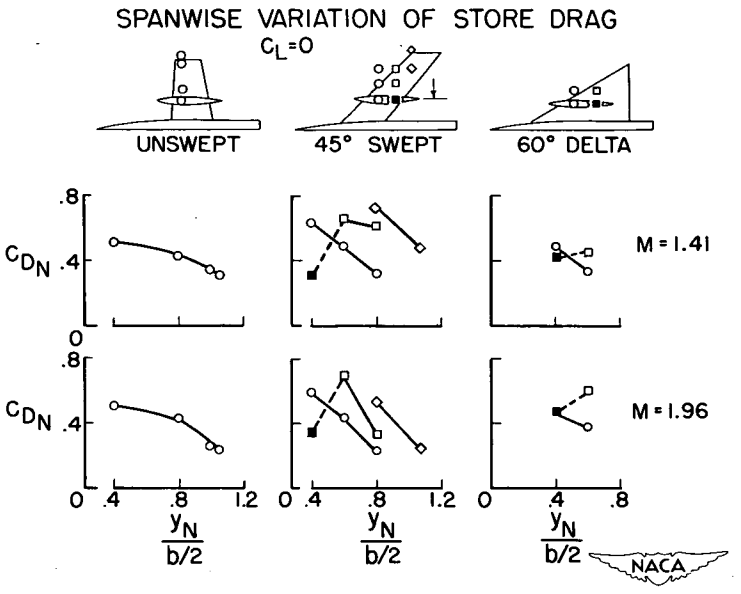

Figure 9

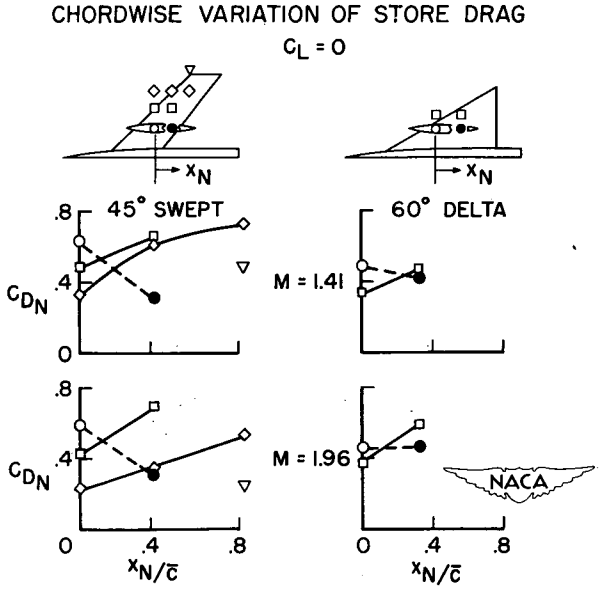

Figure 10

[redacted]

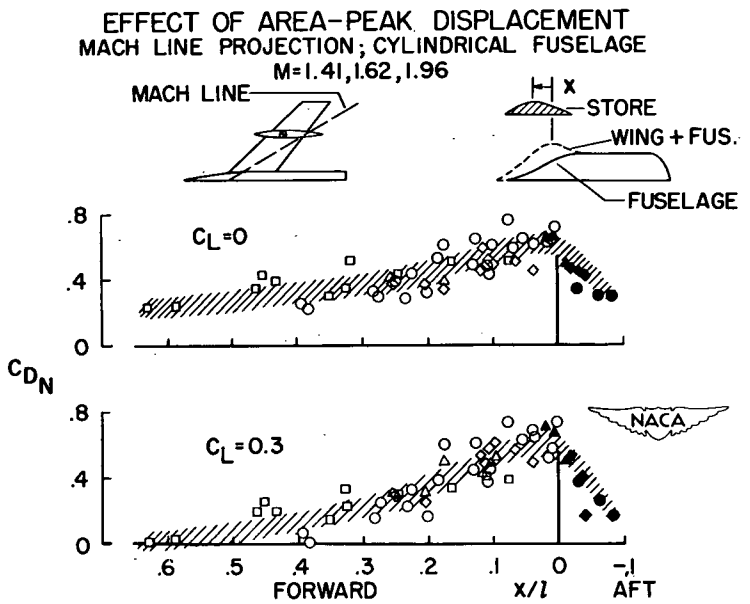

Figure 11

NACA-Langley - 10-29-53 - 325